THE ASTRONOMICAL JOURNAL VOLUME 114, NUMBER 3 SEPTEMBER 1997

ORBITS OF DETACHED MAIN-SEQUENCE ECLIPSING BINARIES OF TYPES LATE F TO K. II. UV LEONIS, UV PISCIUM, AND BH VIRGINIS

DANIEL M. POPPER

Division of Astronomy, University of California, Los Angeles, California 90095-1562
Electronic mail: popper@bonnie.astro.ucla.edu

Received 1997 May 5; revised 1997 June 6

ABSTRACT

This is the second paper in a program to determine fundamental properties of main-sequence stars of types late F to K. Improved spectroscopic orbits are derived for the short-period detached eclipsing binaries UV Leo (G0+G2), UV Psc (G5+K3), and BH Vir (F8+G5). The spectra are obtained with the high-resolution Hamilton spectrometer on the 3 m Shane reflector of the Lick Observatory. A considerable body of photometry is available for each of the three systems, so that photometric parameters are known, allowing the properties of the stars to be evaluated with some confidence, despite intrinsic variations, presumably from star spots. The K3 secondary of UV Psc has a mass of 0.76 $\mathcal{M}_\odot$, the smallest published in this series, although the secondaries of HP Aur and HS Aqr, binaries without adequate photometry, have masses 0.75 and 0.69 $\mathcal{M}_\odot$, respectively, approaching that of the M dwarf, YY Gem, $\mathcal{M}=0.59\ \mathcal{M}_\odot$. Most of the extant models of structure and evolution in the solar mass range do not extend to masses appreciably below 1 $\mathcal{M}_\odot$ because of the change of physical conditions at lower temperatures. Attempts to fit these models to binaries in which the two components differ appreciably in mass lead to contradictory values of the ages of the two components in each case, the secondaries appearing to be twice as old as the primaries or older. Available series of lower main-sequence models stop short of the 0.8 to 1 $\mathcal{M}_\odot$ region, so that their results are not available for comparison. It appears that the transition between the higher- and lower-mass regimes may be a difficult one because of the change of temperature regimes. © *1997 American Astronomical Society.* [S0004-6256(97)02609-5]

1. INTRODUCTION

This is the second paper in a spectroscopic program designed to provide masses and radii of main-sequence stars of types late F to K, where reliable results have been few. Use of the Hamilton echelle-CCD spectrometer on the 3 m Shane telescope of the Lick Observatory (Vogt 1987) for that purpose has been described in Paper I of this series (Popper 1994) and in a detailed presentation of the methods employed in reducing and analyzing the observations (Popper & Jeong 1994). Preliminary results have been published for a number of systems (Popper 1993, 1995), including the three reported in the present communication. In addition, a progress report on the status of observations of 76 potentially useful systems has been published (Popper 1996). Of the 76, 16 are considered to be promising candidates for mass determination (double-lined systems with at least one component of type late F to K), while 17 additional systems may turn out to be useful.

In the present contribution, definitive spectroscopic orbits are obtained for three relatively bright binaries with periods less than one day, for which orbits based on photographic spectra have previously been published: UV Leo (Popper 1965), UV Psc (Popper 1991), and BH Vir (Abt 1965). For UV Leo and BH Vir, the dispersions used earlier were inadequate for effective resolution of the lines of the components, while for UV Psc, the orbit of the secondary component was derived from measurement only of weak Ca II emission lines, an unsatisfactory condition. In the earlier paper (Popper 1991), the potential advantage of using a cross-correlation technique for UV Psc was stressed. As we shall see, the older spectroscopic orbits require substantial revision in all three cases (cf. Table 5).

The cross-correlation procedure employed for obtaining velocities for double-lined binaries of types late F to K has been thoroughly studied for possible systematic effects (Popper & Jeong 1994). It appears that reliable velocities can be obtained even for spectra in which the rotationally broadened lines of the two components are severely blended with each other.

The three systems of this paper are among the small number for which extensive photometric observations have been obtained and analyzed. Recent references are, for UV Leo, Frederik & Etzel (1996); for UV Psc, Budding *et al.* (1987) and Zeilik (1996); and for BH Vir, Zeilik *et al.* (1990). In these systems, as in other short-period systems containing solar-type stars, there are intrinsic light variations, due presumably to spots on the surface of one or both components. In the photometric analyses, efforts were made to "clean" the photometric observations of the intrinsic variability. The variations give rise to some uncertainty in the photometric solutions.

 0004-6256/97/114(3)/1195/11/$10.00

2. SPECTROSCOPIC ORBITS

In the spectrometer configuration employed, 47 orders lie on a chip having 800×800 15 μm pixels. The range of central wavelengths is 443–680 nm. The scale is 2.50 km s^{-1} at the central pixel throughout, or 3.1 Å mm^{-1} at 550 nm. The projected slit width is 2 pixels. It is essential that the same configuration be employed throughout this program in order that the results of the extensive testing carried out (Popper & Jeong 1994) be applicable. Because of the rotationally broadened lines in our short-period binaries, the recent improvement in the camera optics of the Hamilton spectrometer has no significant effect on the quality of the results.

The radial velocities obtained for UV Leo, UV Psc and BH Vir are listed in Tables 1, 2, and 3, respectively. The midexposure dates of the observations correspond to the mean value of sin θ, where θ is the phase measured from the deeper minimum of the light curve. The exposure times were 20 min or less for all but 2 spectra of UV Leo, 30 min or less for all but 7 of UV Psc, and 25 min or less for all but 4 spectra of BH Vir. The phases in Tables 1–3 are obtained from the following ephemerides:

$$\text{For UV Leo,}\quad \mathrm{JD_{Min}} = 2448332.5349 + 0.600086675\ E,$$

$$\text{for UV Psc,}\quad \mathrm{JD_{Min}} = 2448897.4210 + 0.861046566\ E,\quad \text{and}$$

$$\text{for BH Vir,}\quad \mathrm{JD_{Min}} = 2449495.1934 + 0.81687080\ E.$$

The epochs given are for eclipses of the star with the greater surface brightness, which is referred to, in each case, as the "primary." In the tables, this component carries the subscript 1. The ephemeris for UV Leo is based on the compilation of times of minima since JD 2446500 by Wunder (1995), with the minima observed by Frederik & Etzel (1996) added. Minima of UV Psc have been listed by Milano *et al.* (1986), Ibanoglu (1987), Wunder *et al.* (1992), and by Jassur & Kermani (1994). The period employed is based on recent minima in these listings. Rather than try to evaluate a most probable epoch from these minima, radial velocities of UV Psc are sufficiently numerous to define an epoch to ±0.0005 days, which is employed. In the case of BH Vir, Scaltriti *et al.* (1985) concluded that there had been no period variation since 1955. Use of their ephemeris leads to systematic effects in the velocity residuals, which are removed by adjusting their epoch by +0.0087±0.0010 days, which is the epoch listed above. No effort has been made to improve the period for any of the three systems in the range of time covered by the radial velocities.

The nature of the observational material employed for deriving the velocities listed in Tables 1–3 is shown in Figs. 1–6. In Figs. 1–3, spectra of two typical orders among the 40-odd included are shown for each binary as well as the corresponding cross-correlation functions (ccfs), obtained with the use of a G-type star of standard velocity as template, chosen from the lists of Mayor & Maurice (1985). Figures 4–6 show the scatter among the velocities in the different orders for a typical observation of each binary.

TABLE 1. Velocities in UV Leo.

		Observed		Orbital[a]		O–C[b]	
JD-2400000	Phase	V_1	V_2	V_1	V_2	V_1	V_2
48312.8694	0.2289	−174.2	155.0	−175.3	154.7	−4.3	+3.5
48343.7958	0.7655	146.0	−183.7	146.2	−184.3	0.0	−4.7
48345.8458	O.18186	−167.1	141.9	−168.4	141.0	−10.5	+3.5
48345.9153	0.3047	−167.7	151.6	−168.6	151.2	−3.2	+8.3
48611.9939	0.6977	133.9	−168.3	133.6	−169.0	−4.8	+2.5
48612.0130	0.7296	146.8	−177.0	146.8	−177.7	+1.1	+1.3
48612.0358	0.7676	145.9	−176.2	146.1	−176.8	+0.1	+2.6
48612.0524	0.7952	143.9	−170.7	143.9	−171.2	+3.3	+2.5
48699.8705	0.1376	−133.2	113.7	−134.8	111.7	−0.6	−1.1
48699.8871	0.1652	−152.0	125.5	−153.3	124.2	−3.0	−5.4
48699.9016	0.1894	−166.4	141.9	−167.6	141.2	−6.6	+0.5
48699.9167	0.2146	−169.8	148.4	−171.0	147.8	−2.5	−0.8
48909.0285	0.6839	132.8	−161.6	132.1	−162.5	−1.3	+3.7
48909.0378	0.6994	136.2	−168.9	135.9	−169.6	−3.1	+2.4
48909.0472	0.7151	143.7	−175.3	143.5	−176.0	+0.4	+0.4
48909.0558	0.7294	145.3	−173.2	145.3	−173.9	−0.3	+5.1
49116.6548	0.6777	132.4	−170.7	131.7	−171.6	+0.9	−8.1
49116.6856	0.7291	144.2	−181.1	144.2	−181.8	−1.4	−2.8
49116.7348	0.8111	135.8	−173.0	135.6	−173.6	+0.2	−5.3
49382.8633	0.2945	−163.3	142.4	−164.1	141.8	+2.1	−4.4
49382.8740	0.3123	−155.0	138.4	−155.9	136.8	+4.4	−3.3
49382.8858	0.3320	−150.8	125.7	−151.7	124.8	0.0	−6.3
49382.8972	0.3510	−136.3	113.5	−137.4	111.9	+4.0	−8.4
49384.9172	0.7172	146.9	−177.0	146.9	−177.7	+3.3	−0.8
49384.9280	0.7352	149.3	−180.8	149.4	−181.1	+3.1	−1.4
49384.9409	0.7567	149.9	−177.6	149.0	−178.3	+2.2	+2.0
49384.9517	0.7747	149.1	−177.5	149.3	−178.1	+4.2	+0.3
49495.6822	0.2988	−164.1	143.5	−164.9	143.1	+0.1	−1.8
49495.6842	0.3188	−157.3	138.0	−158.2	137.3	−0.5	0.0
49495.7123	0.3490	−133.4	121.8	−134.5	120.2	+8.0	−1.3
49795.7379	0.3224	−157.6	139.5	−158.4	138.7	−2.2	+3.0
49796.8106	0.1070	−117.3	91.0	−119.0	88.3	−6.8	−1.6
49796.8264	0.1333	−138.0	115.3	−139.5	113.4	−8.1	+3.5
50084.9200	0.2200	−164.7	151.8	−165.8	151.5	+3.8	+1.8
50084.9317	0.2395	−166.7	152.6	−167.8	152.3	+4.3	0.0
50084.9471	0.2651	−171.4	159.2	−172.4	159.0	−0.7	+7.1
50084.9612	0.2886	−172.6	158.9	−173.4	158.5	−5.6	+10.7
50084.9999	0.3531	−133.9	117.0	−135.0	115.3	+5.1	−3.6
50086.0888	0.1677	−143.5	124.9	−144.8	123.8	+6.8	−7.1
50086.0964	0.1804	−149.5	134.3	−150.8	133.4	+6.6	−3.6
50176.7818	0.3008	−164.9	148.0	−165.7	147.6	−1.4	+3.4
50176.7964	0.3252	−152.5	138.5	−153.4	137.7	+1.5	+3.3
50178.7807	0.6319	97.5	−133.8	95.7	−134.9	−9.3	+1.7
50178.7960	0.6574	114.7	−145.3	113.5	−146.2	−7.2	+6.8
50178.8125	0.6849	134.8	−164.1	134.2	−164.9	+0.4	+1.8
50178.8297	0.7135	144.3	−178.9	144.1	−179.6	+1.3	−3.6
50178.8433	0.7362	149.8	−179.0	149.9	−179.7	+3.5	+0.1
50178.8601	0.7642	146.4	−180.7	146.6	−181.3	+0.2	−1.6

Notes to TABLE 1

[a]Corrections are applied to the measured velocities from the tests on synthetic binaries (Popper & Jeong 1994) and for proximity effects (Wilson 1990).

[b]Based on the "orbital" velocities and adopted elements (Table 5).

The two components in UV Leo and, to a lesser extent in BH Vir, are similar to each other in mass and radius, while those in UV Psc differ considerably. In addition to blending in the crowded spectra, the lines are rotationally broadened, synchronous rotational velocities being 89 and 83 km s^{-1} for the components of UV Leo, 70 and 53 for UV Psc, and 76 and 69 for BH Vir.

The material in Table 4 relates to the quality of the spec-

TABLE 2. Velocities in UV Pac.

		Observed		Orbital		O–C	
JD-240000	Phase	V_1	V_2	V_1	V_2	V_1	V_2
47398.0041	0.6111	81.9	−92.7	83.1	−91.0	+1.4	+0.2
47399.0008	0.7687	122.6	−146.5	124.2	−146.4	+1.3	−2.1
47407.9386	0.1488	−89.0	124.5	−90.6	122.9	−1.6	−5.4
47785.9329	0.1429	−84.8	125.5	−86.4	123.8	−0.1	−1.0
48523.9144	0.2179	−109.3	159.6	−110.2	158.9	−0.6	+4.1
48523.9206	0.2251	−110.8	160.4	−111.7	159.7	−1.1	+3.6
48523.9275	0.2331	−110.9	160.6	−111.8	159.9	−0.5	+2.8
48611.6663	0.1310	−78.6	120.7	−80.4	118.4	+0.1	+1.0
48611.6890	0.1573	−89.0	133.4	−90.5	132.4	+2.1	−0.5
48611.7112	0.1831	−98.3	145.6	−99.6	144.6	+2.1	−0.1
48611.7422	0.2191	−106.2	160.1	−107.1	159.4	+2.7	+4.3
48821.9315	0.3282	−97.0	138.5	−98.1	137.2	0.0	−2.8
48821.9391	0.3370	−91.9	135.8	−93.8	134.4	+1.0	−1.4
48821.9486	0.3481	−86.4	126.8	−87.7	125.1	+2.6	−4.9
48821.9579	0.3589	−82.0	122.4	−83.5	120.4	+2.0	−3.4
48908.8162	0.2341	−111.7	162.2	−112.6	161.5	−1.2	+4.4
48908.8221	0.2410	−112.6	160.9	−113.5	160.2	−1.7	+2.5
48908.8290	0.2490	−112.8	161.9	−113.7	161.2	−1.7	+3.3
48910.8560	0.6031	76.0	−89.8	77.2	−88.0	+0.2	−2.8
48910.8753	0.6255	87.3	−99.9	88.6	−98.5	−0.9	+2.8
48910.8937	0.6469	97.1	−116.2	98.5	−115.1	−1.4	−0.5
48910.9142	0.6707	106.8	−126.2	108.1	−125.5	−1.3	+1.4
48910.9346	0.6944	114.1	−142.7	115.5	−142.6	−1.1	−6.4
48910.9542	0.7172	120.4	−147.5	121.9	−147.4	+0.6	−5.3
48910.9732	0.7392	122.6	−149.4	124.2	−149.3	+0.7	−4.3
49202.9320	0.8136	110.8	−134.9	112.5	−134.3	−2.0	−0.9
49202.9406	0.8236	107.7	−132.1	109.4	−131.3	−2.0	−1.9
49202.9535	0.8385	101.7	−124.3	103.4	−123.3	−2.6	−0.8
49202.9635	0.8502	98.1	−118.9	99.8	−117.8	−1.4	−1.5
49260.9347	0.1766	−97.6	139.1	−99.0	138.0	+0.7	−4.1
49260.9499	0.1942	−102.4	147.9	−103.6	147.0	+0.2	−1.7
49260.9643	0.2110	−106.4	156.3	−107.5	155.5	+1.0	+2.1
49260.9808	0.2301	−110.0	163.0	−110.9	162.3	+0.2	+5.6
49292.8676	0.2627	−110.1	163.8	−110.9	163.1	+0.7	+5.7
49292.8825	0.2800	−109.2	156.7	−110.1	155.9	−0.2	+0.7
49292.8973	0.2972	−106.0	154.6	−106.9	153.7	0.0	+2.4
49293.7040	0.2341	−112.1	159.6	−113.0	159.2	−1.6	+2.0
49293.7380	0.2736	−111.4	157.8	−112.3	157.0	−1.6	+0.8
49293.7657	0.3058	−104.8	152.7	−105.8	151.7	−1.0	+3.0
49293.7939	0.3385	−94.1	127.6	−95.3	126.1	−1.1	−9.0
49293.8255	0.3752	−77.4	113.3	−79.1	110.8	−1.7	−2.6
49294.8809	0.6009	76.7	−88.9	77.9	−87.1	+2.2	−3.6
49294.9025	0.6260	89.1	−104.9	90.3	−103.4	+0.5	−1.8
49294.9210	0.6475	97.1	−118.0	98.5	−116.9	−1.6	−1.9
49294.9358	0.6647	105.2	−123.2	106.5	−122.5	−0.7	+1.6
49384.6108	0.8112	112.9	−132.3	114.6	−131.7	−0.5	+2.6
49384.6222	0.8244	108.7	−126.4	110.4	−125.9	−0.7	+3.2
49384.6334	0.8375	104.3	−120.8	106.0	−120.0	−0.4	+3.0
49384.6449	0.8508	97.4	−114.0	99.1	−112.9	−1.8	+3.0
49619.9745	0.1573	−90.8	129.2	−92.3	127.8	+0.3	−5.1
49619.9856	0.1702	−95.6	134.5	−97.1	133.3	+0.4	−5.9
49670.7860	0.1686	−96.3	135.1	−97.7	133.8	−0.8	−4.7
49907.9773	0.6372	93.1	−108.4	94.5	−107.1	−0.9	+1.7
49907.9923	0.6546	101.4	−115.0	102.9	−114.1	−0.3	+4.8
50083.6270	0.6328	90.7	−105.6	92.1	−104.3	−1.1	+1.8
50083.6450	0.6537	100.6	−116.8	102.0	−115.9	−0.8	+2.5
50083.6636	0.6753	108.7	−125.7	111.1	−125.1	+0.1	+3.8
50083.6905	0.7066	117.2	−139.6	118.6	−139.2	−0.8	+0.5
50084.5922	0.7538	124.8	−147.3	126.4	−146.7	+2.7	−1.4
50084.6102	0.7747	123.2	−141.0	124.8	−140.9	+2.5	+2.6
50084.6280	0.7954	120.7	−140.1	122.4	−139.8	+3.4	−0.6
50084.6481	0.8187	113.6	−130.8	115.3	−130.2	+2.4	+1.2
50084.6658	0.8392	104.7	−118.0	106.4	−117.1	+0.7	+5.0
50084.6847	0.8612	95.6	−112.0	97.2	−110.7	+1.1	−0.9
50084.7027	0.8821	86.0	−98.6	87.5	−96.9	+2.1	−0.9

See notes to TABLE 1.

TABLE 3. Velocities in BH Vir.

		Observed		Orbital		O–C	
JD-240000	Phase	V_1	V_2	V_1	V_2	V_1	V_2
47253.8310	0.1605	−137.2	110.0	−138.1	110.6	+0.3	−1.2
47696.6829	0.2926	−153.7	129.0	−153.4	129.4	+1.6	−0.8
48023.7354	0.6650	100.7	−147.0	101.4	−147.3	−0.3	+7.0
48079.6818	0.1536	−134.6	109.5	−135.9	109.4	−0.9	+1.3
48080.6842	0.3808	−113.0	85.3	−115.8	86.9	−0.6	+0.8
48081.6775	0.5967	60.2	−111.8	62.3	−114.5	+1.4	−5.3
48822.6722	0.7104	116.3	−172.9	116.6	−172.1	−0.4	−0.8
49383.0448	0.7095	117.7	−171.9	118.0	−171.1	+1.2	0.0
49383.0564	0.7237	119.2	−178.1	119.4	−178.3	0.0	−4.4
49383.0684	0.7384	121.3	−178.0	121.5	−177.2	+0.6	−1.6
49383.0819	0.7549	123.0	−175.6	123.9	−174.8	+2.7	+1.2
49385.0273	0.1364	−122.5	96.4	−124.5	97.3	+1.2	−0.4
49385.0398	0.1518	−131.0	105.8	−132.4	106.5	+1.7	−0.5
49385.0547	0.1700	−141.1	114.4	−141.6	114.8	+1.0	−1.7
49495.7398	.0.6689	101.8	−153.6	102.5	−153.9	−0.9	+2.4
49495.7516	0.6833	107.0	−164.1	107.6	−163.9	−1.5	−1.3
49495.7634	0.6978	114.1	−169.5	113.5	−169.1	−0.3	−1.4
49495.7759	0.7131	117.6	−178.3	117.9	−178.8	+0.4	−6.9
49795.9270	0.1532	−134.6	108.9	−136.1	109.5	−1.3	+1.7
49795.9430	0.1728	−144.3	117.8	−144.8	118.0	−1.0	+0.2
49795.9601	0.1937	−153.7	125.2	−153.7	125.5	−2.4	−0.6
49906.6921	0.7500	120.1	−176.4	120.4	−175.6	−0.9	+0.5
49906.7119	0.7743	116.9	−172.9	117.3	−172.1	−2.4	+2.2
49906.7304	0.7969	115.7	−175.3	116.5	−175.2	+1.3	−5.9
50085.0866	0.1377	−126.4	99.6	−128.4	100.5	−1.9	+2.0
50086.0459	0.3121	−145.7	124.0	−146.1	124.6	+3.4	+0.5
50086.0673	0.3383	−135.0	112.8	−136.6	113.7	+2.4	+1.3
50177.8133	0.6522	90.6	−144.8	91.6	−145.6	−4.0	+2.0
50177.8314	0.6744	104.2	−156.6	104.9	−156.7	0.8	+2.1
50177.8513	0.6987	112.9	−164.6	113.3	−164.2	−0.8	+3.8
50177.8690	0.7204	119.9	−173.7	120.2	−172.9	+1.3	+0.5
50177.8966	0.7542	120.8	−173.0	121.2	−172.2	0.0	+3.8
50177.9160	0.7780	121.4	−173.1	122.0	−172.4	+2.9	+1.3
50265.6810	0.2184	−159.3	129.9	−158.9	130.0	−1.6	−2.7
50265.6928	0.2329	−160.0	135.7	−159.5	135.8	−0.3	+0.9
50265.7050	0.2478	−161.4	135.8	−160.9	135.9	−0.9	+0.1
50265.7183	0.2641	−160.4	134.2	−160.0	134.3	−0.5	−0.9
50265.7301	0.2786	−159.1	133.5	−158.7	133.7	−0.9	+0.4
50265.7412	0.2921	−154.6	129.9	−154.4	130.8	+0.8	+0.4

See Notes to TABLE 1.

troscopic observations: The average number of orders giving usable ccfs, the average dispersion among the velocities in the different orders for each component (the "internal" dispersions), and the rms departure of a velocity from the best fitting velocity curve (the "external" dispersions).

Two small corrections are applied to the individual measured velocities. First are the corrections, shown in Fig. 5 of Popper & Jeong (1994), resulting from an analysis of velocities of synthetic double-lined binaries. Second are corrections resulting from the displacement of the center of mases from the center of light because of the effects of tidal distortion and mutual irradiation of the components. These corrections are provided by a program developed and described by Wilson (1990). The successive sets of velocities are referred to as "observed," "corrected," and "orbital," the last presumably being velocities of the center of mass of each star. Observed and orbital velocities are listed in Tables 1, 2, and 3.

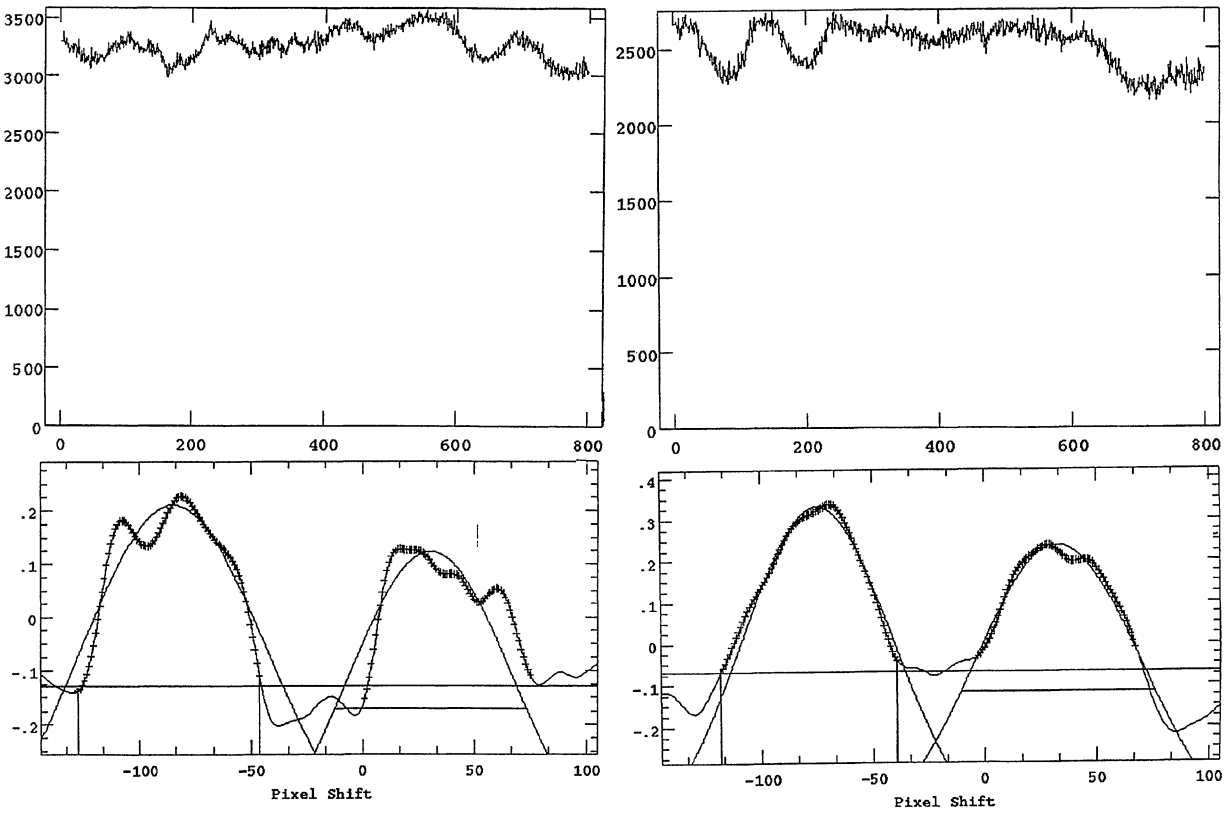

FIG. 1. Above, spectra of UV Leo. Below, the corresponding cross-correlation functions relative to a star of standard velocity as template. On the left, grating order 102, centered at 560.2 nm. On the right, grating order 115, centered at 496.8 nm. Ordinates for the spectra are counts per pixel, summed over the rows of an order. Ordinates for the ccfs are the correlations. The ccfs are fitted with Gaussians. The horizontal lines have no significance. The pixel shifts are relative to the spectrum of the template. One pixel corresponds to 2.50 km s^{-1}. Order 115 is typical of orders giving relatively well-defined ccfs, while order 102 is typical of orders giving less well-defined peaks, particularly for the secondary components. The spectrum was exposed near phase 0.25.

The parameters of circular orbits from all three sets of velocities are listed in Table 5, which also contains the results of the earlier spectrographic observations on photographic plates. The residuals, O–C, in Tables 1–3 are for the "orbital" velocities. Figures 7–9 show the orbital velocities and corresponding velocity curves.

Examination of Tables 1–3 reveals a tendency for the residuals of a given component on a single night to have the same sign more often than expected by chance. This effect is most pronounced for UV Psc, though present in all 3 systems. The effect does not appear to be a consequence of "night errors" in the velocities, since the residuals often have opposite signs for the two components in a given observation. A possible explanation is the presence of large spotted areas on a star, giving rise to an asymmetric surface distribution of light relative to the line of sight. All the systems show intrinsic irregularities in their photometry, which are attributed to star spots. One may hope that there are large enough numbers of spectroscopic observations for the effect of systematic trends in the residuals not to cause systematic departures of the velocity amplitudes, K in Table 5, from their true values. That the external velocity dispersions do not greatly exceed the internal implies that the amplitudes are not significantly affected by the systematic runs of the residuals.

3. PHOTOMETRIC MATERIAL

3.1 UV Leonis

The most recent and thorough discussion of photometry of UV Leo is that of Frederik & Etzel (1996), who also summarize the 4 earlier photometric investigations. As with all solar-type close binaries of short period, the light curve of UV Leo shows intrinsic variations, which, in this binary, appear to have been first noticed by Broglia (1961).

In all photometric studies of UV Leo, the component eclipsed at the deeper minimum is the one shown to have the larger mass. It is also the star found in the earlier photographic spectroscopy (Popper 1965) to have the slightly stronger lines.

The study by Frederik & Etzel (1996, hereafter FE) is the only one incorporating the effects of star spots. These effects are removed in deriving the invariant parameters of the stars. In the FE analysis, the hotter, more massive star (mass ratio 1.043) is the smaller and less luminous one, whereas for two main-sequence stars, the opposite relationship is expected to apply unless mass exchange between the detached components has taken place. In evaluating the light ratio, the key photometric parameter is the ratio of the radii of the components. In a case of partial eclipses of comparable depth, as with UV Leo, the value of this quantity depends critically on

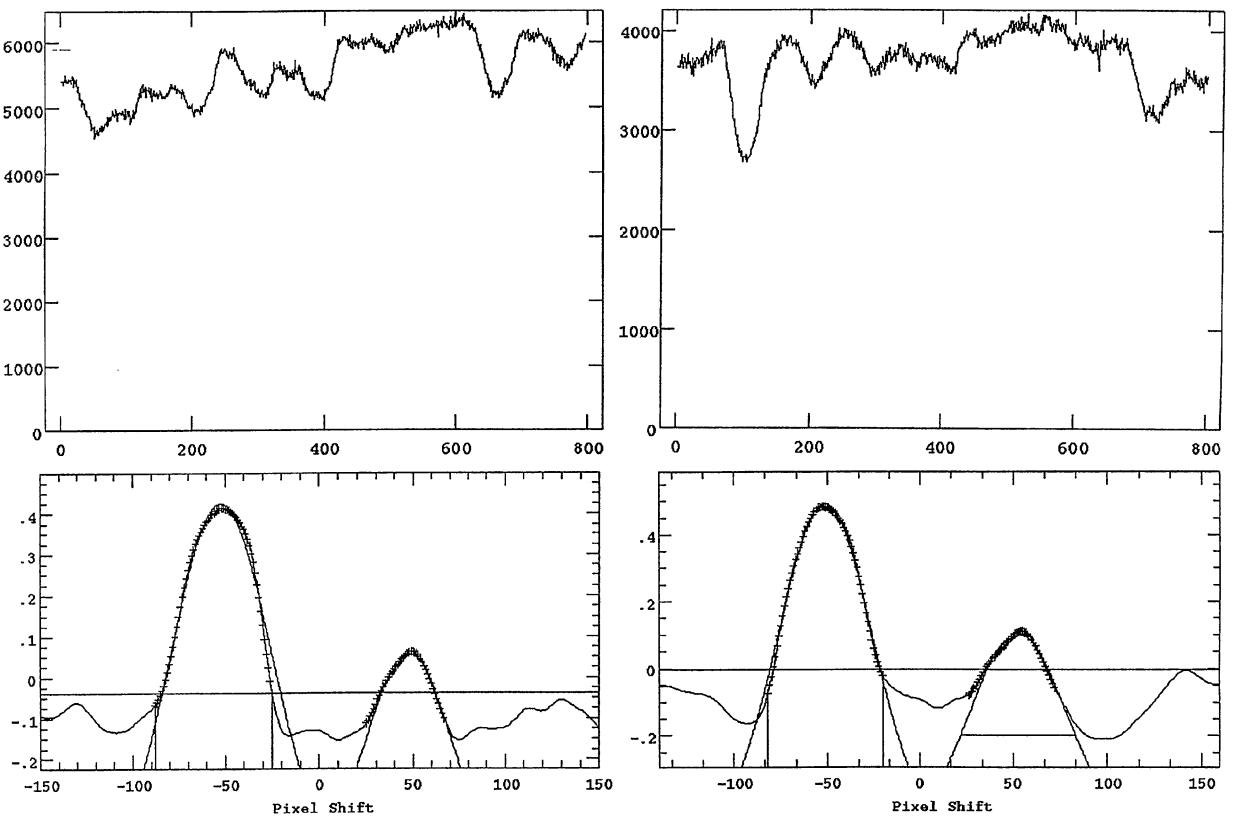

FIG. 2. The same as Fig. 1, for UV Psc.

small details of the shapes of the two minima. Examination of Fig. 2 of FE shows that the observed light curve and the curve corrected for the effects of spots differ from each other by significant amounts. Thus the details of the "cleaned" form of the light variation within minima could be sensitive to the spot model adopted.

In cases of uncertainty, the decision as to which component is the more luminous one can often by made by appealing to the spectrum. In examining my earlier photographic spectra (Popper 1965), I concluded that the cooler, less massive star was "very slightly less luminous," in disagreement with the conclusion of FE. The new spectra support the result from the older ones: The spectrum represented in Fig. 1 was exposed near phase 0.25, when the primary component had a negative orbital velocity. In each of the orders shown, the negatively displaced cross-correlation function (ccf) has a larger area than that positively displaced. Qualitative examination of a random selection of 480 ccfs from spectra observed near both nodes showed the hotter, more massive star to have the larger ccf in 58% of the cases. The conclusion is strengthened by considering that the lines of of a hotter G-type star are intrinsically weaker than those of a cooler one. Further evidence in this matter is based on the widths of the ccfs, which, in the case of synchronous rotation, should be proportional to the radius of the corresponding star. Measurement of the full widths of 520 ccfs of each component, having a considerable variety of intensities and shapes, gives a ratio of radii of 1.065, with the hotter, more massive star being the larger, and hence the more luminous one, again in disagreement with the photometric solution by FE.

I do not consider either of these rather crude pieces of evidence favoring the more massive, hotter star in UV Leo being the larger and more luminous one, to be definitive. Perhaps the best that can be said is that one should accept with caution the conclusion of FE that the components of UV Leo have had a tortured evolutionary history.

Earlier the question was raised as to the possible influence upon a light curve of the procedure employed in correcting it for the presence of dark star spots. The spot model employed by FE places two spots on the outer hemisphere of the cooler star. There has been considerable discussion in recent years on the question of whether the widely used model with one or two large spots, often lying in the polar region, is a realistic model, and whether a model more nearly resembling the solar distribution of spots might be preferable. It should be pointed out that, if the light curve is depressed relative to the unspotted curve for a full orbital period or more, and if the depression is attributed to one or two spots, their position must lie in the polar region of an edge-on binary, since that is the only region in which the spots would never disappear. If, on the other hand, the model contains a considerable number of smaller spots nearer the equator, those rotating out of sight could be replaced by others coming into view, keeping the depression approximately constant. Models of this latter kind have been proposed recently by Kürster *et al.* (1994), by Eaton *et al.* (1996), and by Alekseev & Gershberg (1996).

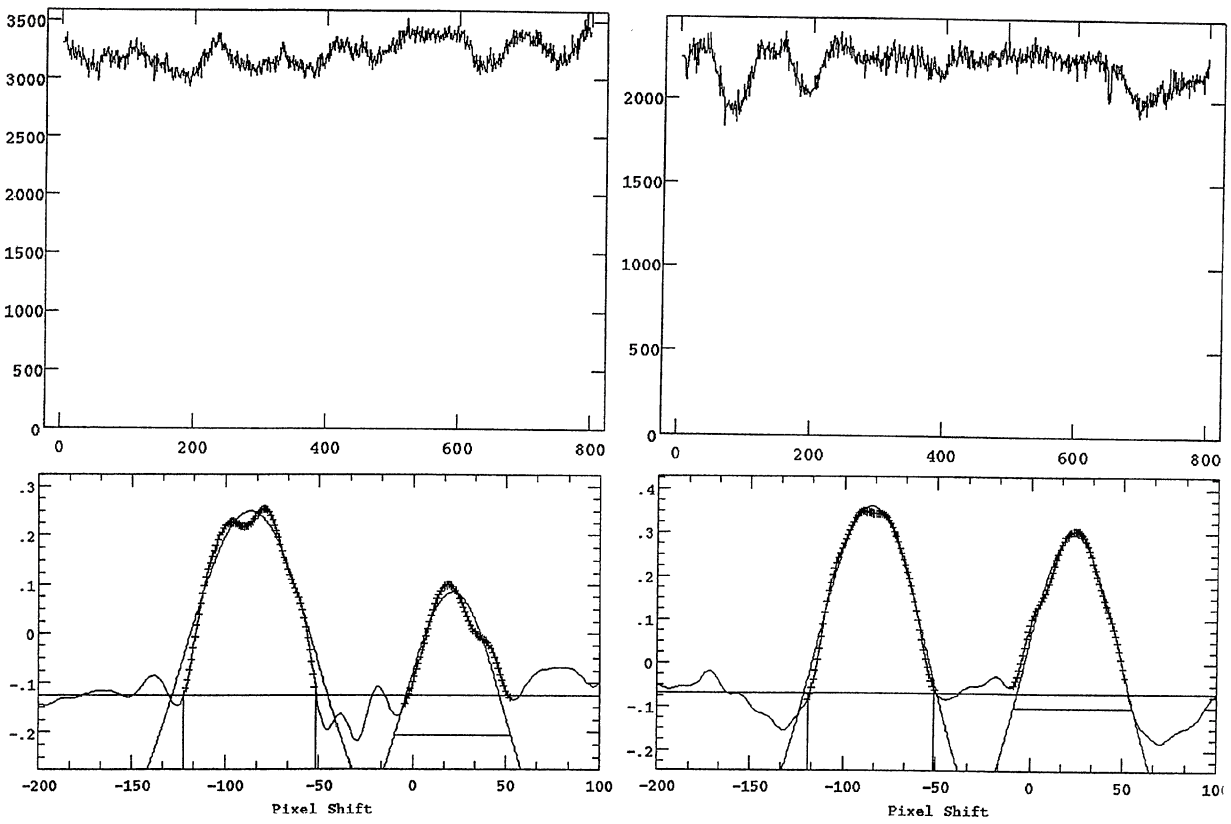

FIG. 3. The same as Fig. 1, for BH Vir.

References to the earlier literature in this field, in some of which the importance of Doppler imaging is stressed, may be found in Eaton *et al.* See also Budding & Zeilik (1994). Without carrying out actual tests on the FE photometry, it is not possible to ascertain the extent to which the star-spot model employed may influence the photometric solution and perhaps resolve the discrepancy between the photometric and spectroscopic results on the sense of the luminosity ratio of the components of UV Leo.

Because of the uncertainty in the photometric solution, the differences in radius and luminosity of the components of UV Leo are not well determined. On the other hand, the orbital inclination (83°), average relative radius, r, (0.29 ± 0.005), and mean color index ($B-V=0.624\pm0.01$) appear to be well established. FE deduce "unspotted" colors 0.60 and 0.63, corresponding to types G0 and G2.

3.2 UV Psc

Zeilik *et al.* (1996) and Budding *et al.* (1996) have analyzed 14 light curves of UV Psc, observed by various persons, using the single star-spot model (Budding & Zeilik 1987). The components differ from each other appreciably, their adopted light ratio in the V band being 5.6 ± 0.7, so that there is no potential ambiguity of the kind encountered in UV Leo. (See above.) The agreement among the 14 solutions is quite good, the standard deviation of a single value being 0.028 for k (the ratio of the radii), 0.008 for r_1, and 1.1° in

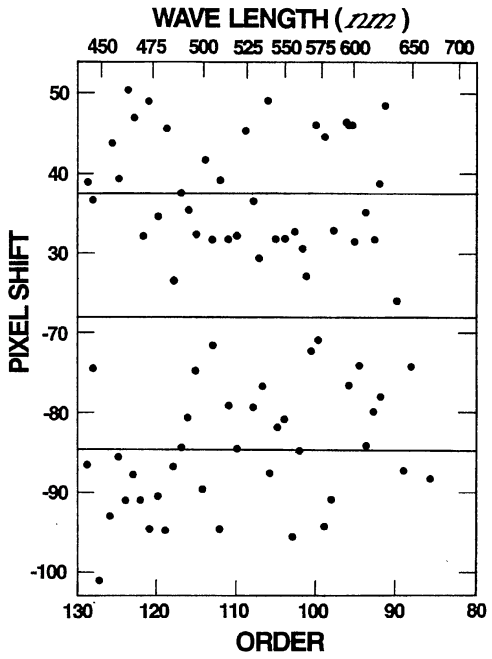

FIG. 4. Pixel shifts in a typical spectrum of UV Leo, relative to the spectrum of a star of standard velocity. Above, primary component; below, secondary. One pixel corresponds to 2.50 km s^{-1}. The horizontal line in each panel shows the mean pixel shift, from which the relative velocity is obtained.

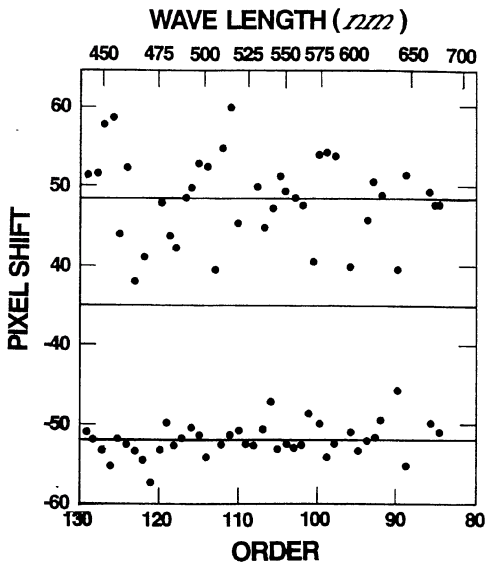

FIG. 5. The same as Fig. 4, for UV Psc, except that the primary component is below.

i. The average values are $k=0.752\pm0.017$, $r_1=0.242\pm0.005$, and $i=88.9°\pm2.0°$. These values are adopted pending a study based on an alternate star-spot model referred to in the discussion of UV Leo above. While the geometric parameters listed are similar to those adopted in my earlier discussion of a much more limited set of photometric observations (Popper 1996), the radiative parameters (light ratio, surface-flux ratio, color indices) are subject to considerable uncertainty. The color index of the combined light, $B-V=0.73$, corresponds to a main-sequence type of G8. My evaluation from spectra in the photographic region (Popper 1991), where the dominance of the hotter star is greater than in the V band, is G5, whereas the strength of the Na D lines in the visual spectrum corresponds to G9. The light ratio in the V band, quoted above, combined with the ratio of the radii, leads to a value of the flux-ratio parameter, $\Delta F'_v=0.125\pm0.015$, where $\Delta F'_v=1/4\log(J_1/J_2)_v$, J being the surface brightness. This value of $\Delta F'_v$ corresponds to a value of $\Delta(B-V)$ of 0.39 ± 0.05, where, for consistency with earlier work, I have retained the flux scale derived from the Bell & Gustafsson analysis (1989). The value of $\Delta(B-V)$ given by the mean light ratios in V and B in the Zeilik *et al.* compilation is 0.37, in excellent agreement with that derived

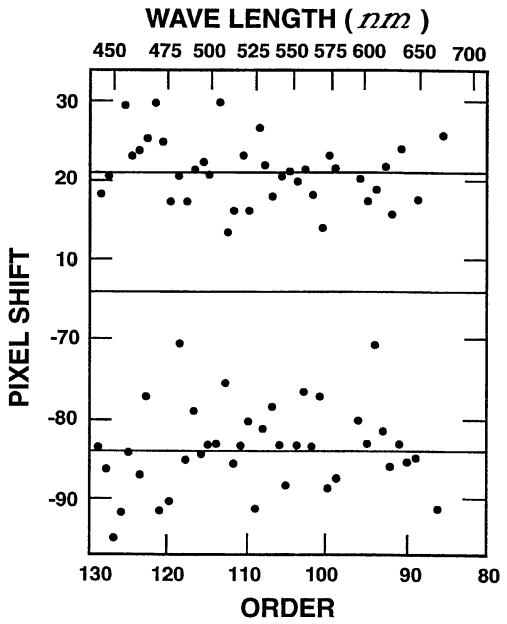

FIG. 6. The same as Fig. 4, for BH Vir.

TABLE 4. Statistics on the Spectra.

	UV Leo		UV Psc		BH Vir	
	Pri	Sec	Pri	Sec	Pri	Sec
Number of spectra	49	49	65	65	39	39
Average number of orders	36	37	41	36	40	37
Average interal velocity dispersion (km s^{-1})[a]	3.2	3.0	0.85	2.1	1.9	2.1
Average external velocity dispersion (km s^{-1})[b]	4.5	4.1	1.5	3.4	1.6	2.7

Notes to TABLE 4

[a]Among the orders.
[b]Relative to the adopted orbit.

TABLE 5. Circular orbits.[a]

	UV Leo		UV Psc		BH Vir	
	Pri	Sec	Pri	Sec	Pri	Sec
			Observed			
V_0	−12.2	−13.0	5.7	6.3	−19.3	−20.4
	±0.6	±0.6	±0.2	±0.4	±0.3	±0.4
K	159.3	166.6	116.1	152.8	140.3	156.0
	±0.7	±0.6	±0.4	±0.5	±0.3	±0.5
σ	4.2	4.0	1.5	3.4	1.6	2.7
			Corrected[b]			
V_0	−13.0	−13.8	5.9	6.4	−19.3	−20.2
	±0.6	±0.7	±0.2	±0.4	±0.3	±0.4
K	159.0	165.9	117.6	151.7	140.5	155.7
	±0.7	±0.6	±0.2	±0.6	±0.3	±0.5
σ	4.2	4.1	1.5	3.4	1.6	2.7
			Orbital[c]			
V_0	−12.7	−13.9	5.9	6.3	−19.4	−20.1
	±0.6	±0.6	±0.2	±0.4	±0.3	±0.4
K	159.7	166.5	117.9	151.6	140.7	155.9
	±0.7	±0.6	±0.2	±0.5	±0.3	±0.5
σ	4.5	4.1	1.5	3.4	1.6	2.7
			Previously published[d]			
V_0	−18:	...	7	6	−29	...
K	150	161	120	167	138	135
	±2	±3	...	...	...	...
σ	...	...	3	5	8	15

Notes to TABLE 5

[a]All quantities are in km s^{-1}.
[b]Corrected on the basis of tests with synthetic binaries (Fig. 5 in Popper & Jeong 1995).
[c]Velocities of b corrected for the effects of mutual irradiation and tidal distortion (Wilson 1990). Adopted values.
[d]UV Leo, Popper (1965); UV Psc, Popper (1991); BH Vir, Abt (1965).

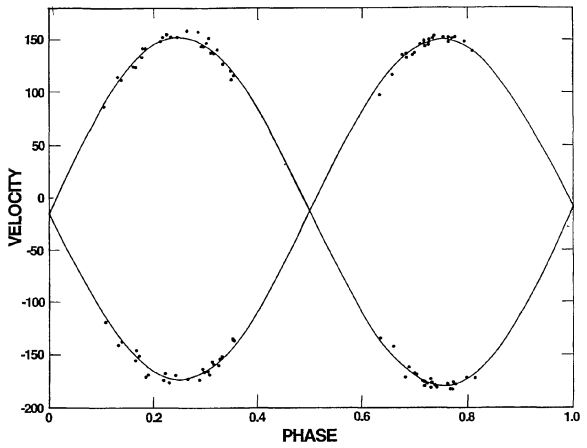

FIG. 7. Radial velocities of the components of UV Leo and velocity curves based on the adopted circular elements (Table 5).

from the adopted ratios of light and radius and the flux scale. The observed data are satisfied by individual color indices, $B-V$, of 0.65 ± 0.02 and 1.04 ± 0.07, corresponding to types G5 and K3. The uncertainties listed are based on the scatter among the individual data sets listed by Zeilik *et al.* (1996), a not particularly satisfactory treatment. The extent to which choice of a star-spot model may lead to systematic effects in the light-curve solution is an additional source of uncertainty.

In my earlier discussion of the radiative properties of the components of UV Psc (Popper 1991), the extensive work of Zeilik *et al.* (1996), in which a considerable number of light curves were "cleaned" of the effects of star spots, was not available. Hence the present evaluation of $\Delta F'_v$ and the corresponding values of the color indices derived here should be on a sounder basis.

3.3 BH Vir

Zeilik *et al.* (1990) have also analyzed the photometric observations of BH Vir available to them. Subsequently, analyses employing the star-spot model have appeared by Zhai *et al.* (1990), by Heckert & Summers (1995), and by Clement *et al.* (1996, preprint). There are no serious dis-

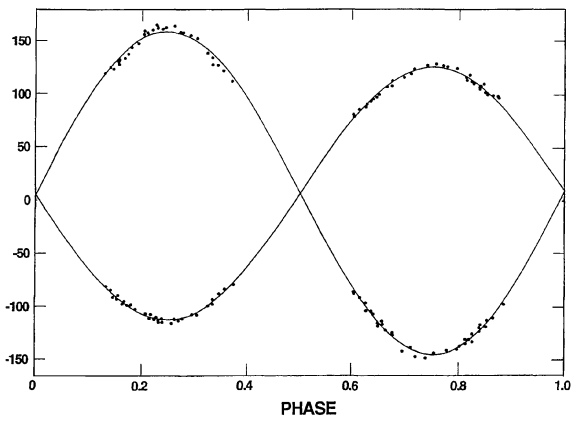

FIG. 8. As Fig. 7, for UV Psc.

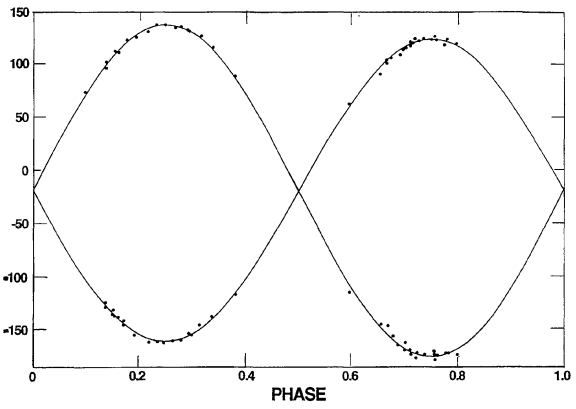

FIG. 9. As Fig. 7, for BH Vir.

agreements among the derived values of the geometrical elements, for which one may adopt $k=0.91\pm0.02$, $r_1=0.26\pm0.005$, and $i=87°\pm0.5°$. The uncertainties given reflect the agreement among the results of the different investigations. There is also reasonable agreement among the values of the radiative parameters in the V band: $L_1/L_2=1.85\pm0.10$, $\Delta F'_v=0.045\pm0.005$. The last value corresponds to a difference in $B-V$ of 0.16 ± 0.02. Three values of $B-V$ in the combined light have been published: Popper & Dumont (1977), 0.54; Lacy (1979), 0.57; and Scaltriti *et al.* (1985), 0.615. Lacy's observations have the most weight. He also observed BH Vir at secondary minimum when the light of the larger, hotter component dominates, finding $B-V=0.52$. We may adopt for the two components 0.51 and 0.67, corresponding to types F8 and G5. The strength of the Na D lines in the combined spectrum corresponds to F9.

4. DISCUSSION

The properties of the components of the three binaries, derived from the material discussed in Secs. 2 and 3, are contained in Table 6.

In two previous communications (Popper 1995, 1996), I have discussed the status of the spectroscopic program designed to increase our meager supply of fundamental properties of main-sequence stars of solar mass or less. As pointed out in these references, there is a considerable number of promising systems. The first two papers of the current series (Popper 1994 and the present paper) contain analyses of RT And, CG Cyg, UV Leo, UV Psc, and BH Vir. The results for these systems augment significantly the supply of data in the late F to K range contained in Andersen's (1991) review. Hence, it may be appropriate at this time to examine briefly the available material for stars with masses less than 1.5 $\mathcal{M}_\odot$ contained in Table 1 of Andersen (1991), Table 5 of Popper (1994), and Table 6 of this paper[1] in the

[1]The following errors in these table may be noted: The radius of EW OriB (Andersen 1991) should be 1.091 rather than 1.145. The corrected value of $\log L$ is 0.08 and of M_v 4.59. In Table 5 of Popper (1994), all the values of M_v in the last column are incorrect. The correct values are, for RT And, 4.99 and 5.75 and for CG Cyg, 5.06 and 5.65. The listed values of $\log L$ are correct.

TABLE 6. Properties of the components.

	UV Leo	UV Psc		BH Vir	
	Average	Hotter	Cooler	Hotter	Cooler
Mass ($\mathcal{M}_\odot$)	1.105±0.012	0.975±0.009	0.76±0.005	1.165±0.008	1.052±0.006
Radius ($R_\odot$)	1.13±0.02	1.11±0.02	0.83±0.03	1.25±0.025	1.14±0.025
log g (cgs)	4.374±0.020	4.335±0.016	4.480±0.031	4.34±0.02	4.35±0.02
$B-V$	0.62±0.02	0.65±0.02	1.04±0.03	0.51±0.02	0.67±0.03
log T_e	3.767±0.025	3.762±0.007	3.677±0.007	3.785±0.008	3.742±0.016
log L ($L_\odot$)	0.13±0.02	0.09±0.03	−0.50±0.04	0.28±0.03	0.09±0.06
M_V	4.48±0.05	4.58±0.10	6.39±0.20	3.92±0.20	4.58±0.20

log R–log $\mathcal{M}$ plane (Fig. 10) and in the log L–log $\mathcal{M}$ plane (Fig. 11). The components of the visual binary, α Cen are included. This is the only visual binary with properties known with a precision comparable to that of the better determined eclipsing binaries. The M dwarfs, YY Gem and CM Dra, are outside the range of this study. Of the three properties, the masses are derived most directly from observational data, the radii less so, since they depend, in addition, on solution of a light curve. Nevertheless, both of these quantities are thought to be known to an accuracy of 2% or better in almost all cases. The luminosities are the least directly determined, since they require, in addition to the radii, the effective temperatures, which, in turn, depend on color indices as well as on the flux ratios, both of which may be subject to considerable uncertainty. Also shown in Figs. 10 and 11 are the loci for the start and termination of core hydrogen burning from the models of Schaller *et al.* (1992) for $Y=0.30$, $Z=0.02$. Added in Fig. 10 are three isochrones based upon the Schaller *et al.* models. These models are chosen arbitrarily and for convenience, without attempting to evaluate the merits of different sets of models. The lower limit of masses in Schaller *et al.* (1992), 0.8 $\mathcal{M}_\odot$, is close to the 0.76 of the lowest mass in the compilation, that of the secondary of UV Psc.

As new knowledge is obtained, the details of interior models are subject to alteration. In this sense, a comparison of observations with theoretical models is never definitive. Much of the material represented in Figs. 10 and 11 has not hitherto been subjected to comparison with models. In this context it is assumed that the curves in Fig. 10 may serve as a suitable starting point of a brief and simple discussion.

First, we note that nearly all the stars lie within the theo-

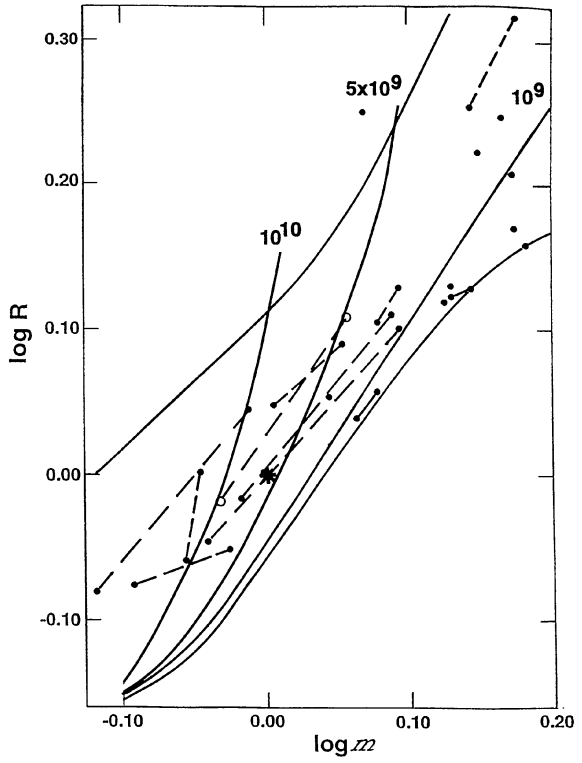

FIG. 10. Binaries in the mass-radius plane. Solid dots represent the components of eclipsing binaries, while the open circles are for the visual binary, α Cen. The asterisk is for the Sun. Dashed lines connect the components of a binary. Isolated points are for binaries in which the two components have nearly the same mass and radius or are for the secondaries of binaries for which the primary lies outside the confines of the figure. The curves are based on the models of Schaller *et al.* (1992) for $Y=0.30$, $Z=0.02$. The outer curves are for the beginning and ending of core hydrogen burning. Isochrones are labeled in years.

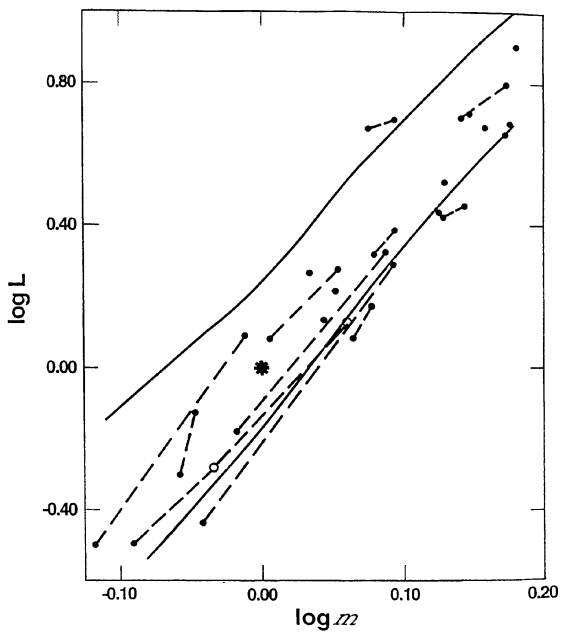

FIG. 11. Binaries in the mass-luminosity plane. Points and curves are as in Fig. 10. Isochrones are not shown.

TABLE 7. Ages estimated from isochrones in the log R—log $\mathcal{M}$ diagram.

Star	log $\mathcal{M}(\mathcal{M}_\odot)$	log $R(R_\odot)$	age (gyr)[a]
FL LyrA	0.087	0.108	1.5
B	−0.018	−0.017	6
RT AndA	0.093	0.100	1
B	−0.041	−0.046	7
UVPscA	−0.011	0.045	9
B	−0.119	−0.081	>20
α CenA	0.057	0.105	4
B	−0.032	−0.025	8

[a]Based on the models of Schaller *et al.* (1992) for $Y=0.70$, $Z=0.02$.

retical main-sequence of Fig. 10. See Andersen (1991) for discussion of this point. Second, the slopes of the lines in Fig. 10 connecting the components of those binaries having components with appreciably different masses, lie within a rather narrow range. There are two prominent exceptions, both among the stars of lower mass. The steepest slope is that for HS Aur. The photometry of this system and its analysis (Popper *et al.* 1986) are sufficiently insecure, particularly in the ratio of the radii, to permit that ratio to be more nearly concordent with the well-determined ratio of the masses than the adopted value. In the case of CG Cyg, the binary with the smallest slope in Fig. 10, the adopted ratio of the radii is closer to unity than expected for the mass ratio.

The rather small range of slopes of most of the lines in Fig. 10, connecting the components of a binary, matches more nearly the ZAMS slope than it does the slopes of the isochrones covering the region of the log R–log $\mathcal{M}$ diagram where most of the stars lie. This disagreement presents something of a dilemma. Since the rate of growth of a radius is strongly dependent on mass, one would expect the slope to increase with the age of a binary. The locations of the stars in Fig. 10 are well above the ZAMS line and, for the most part, above the 1 Gyr locus, a result implying that they are evolved. That the expected increase in slope is not found implies, if interpreted in terms of the models in question, that the more massive star is younger than the less massive. Thus the dilemma. Put another way, the observed slopes of the log R–log $\mathcal{M}$ line for the binaries are, for the most part, considerably smaller than the slopes of the isochrones from the models.

On the observational side, the approximate homogeneity of slopes among most of the binaries cannot result accidentally. Thus, since the masses are known unambiguously, the conclusion is that the adopted radii, despite difficulties from intrinsic variability and differences among different photometric analyses, are not far from their correct values. Exceptions may be the two systems, HS Aur and CG Cyg discussed above.

The nature of the problem may be illustrated quantitavely by evaluating the ages of the stars in the systems with the largest differences in mass between the components: FL Lyr RT And, UV Psc, and α Cen. The results are given in Table 7. Use of different compositions or different opacity tables, for example, will lead to different values for the ages, but it does not appear likely that the apparent discrepancies of age will disappear. For example, the models of VandenBerg & Laskarides (1987) lead to ages roughly twice those in Table 7, but the nature of the discrepancies between the components is about the same.

A difficulty arises in attempting to intrepret observations in the mass range below one solar mass. One is approaching from above the lower limit of masses covered by the models. For example, the lower mass limit of the Schaller *et al.* (1992) models is 0.8 $\mathcal{M}_\odot$. On the other hand, 0.8 $\mathcal{M}_\odot$ is the upper limit of the lower-mass models of Chabrier & Baraffe (1997). Thus there does not appear to be a homogeneous set of models covering just that region of the main sequence that this program is intended to address. As pointed out to me by Roger Ulrich and by Isabelle Baraffe, there are good reasons for the difference in treatment of the higher- and lower-mass regimes. As the temperature decreases, sources of opacity change as do the nature of the core-envelope interface, treatment of the outer boundary condition, perhaps the mixing-length parameter, and even the equation of state.

Ms. Baraffe informs me that she can fit the mass and radius of UV PscB, the star of lowest mass in Figs. 10 and 11 and in Table 7, with solar metallicity and an age of 15 Gyr. The Chabrier & Baraffe (1997) models do not reach the mass of the primary of UV Psc, so the fit is not known. Further, 15 Gyr seems somewhat old for a low-velocity star with Population I composition.

It is natural that model builders have particular problems in mind: globular cluster turnoff point, lower limit of hydrogen-burning, luminosity function for the halo, HR diagrams for different populations, population synthesis, etc., rather than providing comprehensive coverage of parameter space in the models. The observations discussed here show that another region of that space requires thorough treatment and comparison with observations before we can say that the physics of stars on the lower main sequence, below one solar mass, is well understood.

5. SUMMARY

The principal contribution of this paper, as well as its predecessor (Popper 1994) and potential successors, lies in the spectroscopic orbits of the binaries and the resulting masses. A gradual extension of the realm of well-established masses to lower main-sequence values is under way. It is possible that the radii of the stars investigated are known with acceptably small uncertainties, despite their intrinsic variability. The temperatures and luminosities are less certain. In the case of UV Leo, there may be some confusion over which of the nearly equal components is the larger one. Photometric analyses might be improved by adopting a starspot model having a distribution of spots more nearly resembling the solar distribution than a model with one or two large spots, as is generally used. In any event, in order to "clean" a light curve of the effects of intrinsic variability, it is essential to have photometric coverage over a considerable number of orbital cycles, as is available for the 5 systems studied in this paper and its predecessor and discussed pri-

marily in contributions by Zeilik, Budding, and their collaborators. As an aside, it would be particularly beneficial if intensive photometry were applied to the important 9.8 day late G eclipsing binary, HS Aur, which has inadequate photometry as yet (Popper *et al.* 1986), despite its inclusion in Andersen's (1991) critical compilation.

The present paper includes a brief discussion of the available fundamental data on stars of mass 1.5 $\mathcal{M}_\odot$ or less. A serious dilemma appears to be present in the comparison of fundamental stellar properties derived form observations and the predictions of stellar models. In particular, for those binaries having components differing appreciably in radius and mass, it does not appear possible to place the two components on the same isochrone, the less massive components appearing to have greater ages than the more massive by factors of two or more. It may well be that the models employed here are not satisfactory for masses below 0.9 $\mathcal{M}_\odot$ or so, where observations are accumulating for the first time. This range of masses enters the realm of lower temperatures where sources of opacity, the nature of the stellar core, treatment of the outer boundary condition, change in the mixing-length parameter and/or the equation of state employed may lead to different relationships among the fundamental parameters. Thus, when models extending into the 1 solar mass range from below become available, a more meaningful test of stellar theory may be possible. Until that time one might exercise caution in assuming that our understanding of lower main-sequence stars is satisfactory.

It is clear that on both the observational and on the theoretical sides, effort should be placed on main-sequence stars on the range 0.6–0.9 $\mathcal{M}_\odot$ where possible. Attention is directed particularly to the secondaries of HP Aur and HS Aqr (HD 197010) (Popper 1995), with masses approximately 0.75 and 0.69 $\mathcal{M}_\odot$, respectively.

Helpful discussions with Roger Ulrich and Isabelle Baraffe are acknowledged. This program is supported by a grant from the National Science Foundation.

REFERENCES

Abt, H. A. 1965, PASP, 77, 367
Alekseev, I. Yu., & Gershberg, R. E. 1996, Astron. Reports, 40, 528
Andersen, J. 1991, A&AR, 3, 91
Broglia, P. 1961, MSAI, 32, 43
Budding, E., Butler, C. J., Doyle, J. G., Etzel, P. B., Olah, K., Zeilik, M., & Brown, D. 1996, Ap&SS, 236, 215
Budding, E., & Zeilik, M. 1987, ApJ, 319, 827
Budding, E., & Zeilik, M. 1994, Ap&SS, 222, 181
Chabrier, G., & Baraffe, I. 1997, A&A (in press)
Clement, R., Reglero, V., Garcia, M., & Fabregat, J. 1996, preprint
Eaton, J. A., Henry, G. W., & Fekel, F. C. 1996, ApJ, 462, 888
Frederik, M., & Etzel, P. B. 1996, AJ, 111, 2081
Heckert, P. A., & Summers, D. L. 1995, Inf. Bull. Var. Stars, No. 1995
Ibanoğlu, C. 1987, Ap&SS, 139, 139
Jassur, D. M. Z., & Kermani, M. H. 1994, Ap&SS, 219, 351
Kürster, M., Schmitt, I. H. M. M., & Cutispoto, G. 1994, A&A, 289, 899
Lacy, C. H. 1979, ApJ, 228, 817
Mayor, M., & Maurice, E. 1985, in Stellar Radial Velocities, IAU Colloquium 88, edited by A. G. D. Philip and D. W. Latham (Davis, Schenectady), p. 299
Milano, L., Mancuso, S., Vittone, A., D'Orsi, A., & Marcozzi, S. 1986, Ap&SS, 124, 83
Popper, D. M. 1965, ApJ, 141, 126
Popper, D. M. 1991, AJ, 102, 699
Popper, D. M. 1993, ApJ, 404, L67
Popper, D. M. 1994, AJ, 108, 1091
Popper, D. M. 1995, Inf. Bull. Var. Stars, No. 4185
Popper, D. M. 1996, ApJS, 106, 133
Popper, D. M., & Dumont, P. J. 1977, AJ, 82, 216
Popper, D. M., & Jeong, Y.-C. 1994, PASP, 106, 189
Popper, D. M., Lacy, C. H., Frueh, M. L., & Turner, A. E. 1986, AJ, 91, 382
Scaltriti, F., Collins, A., & Busso, M. 1985, A&A, 149, 11
Schaller, G., Schaerer, D., Meynet, G., & Maeder, A. 1992, A&AS, 96, 255
VandenBerg, D. A., & Laskarides, P. G. 1987, ApJS, 64, 103
Vogt, S. S. 1987, PASP 99, 1214
Wilson, R. E. 1990, ApJ, 356, 613
Wunder, E., 1995 Inf. Bull. Var. Stars, No. 4179
Wunder, E., Wieck M., Killing, B., Gulman, Ö., Tunca, Z., & Evren, S. 1992, Inf. Bull. Var. Stars, No. 3760
Zeilik, M. 1996, private communication
Zeilik, M., Ledlow, M., Rhodes, M., Arevalo, M. J., & Budding, E. 1990, ApJ, 354, 352
Zhai, D.-S., Qiao, G.-J., & Zhang, X.-Y. 1990, A&A, 237, 148